Nanoscale

ROYAL SOCIETY OF CHEMISTRY

MINIREVIEW

View Article Online
View Journal | View Issue

Cite this: *Nanoscale*, 2025, **17**, 774

Chirality generation on carbon nanosheets by chemical modification

Ryo Sekiya, *[a,b] Saki Arimura,[a] Haruka Moriguchi[a] and Takeharu Haino *[a,c]

Chirality is an intriguing property of molecules, and an exciting area of study involves the generation of chirality in nanographenes (NGs), also known as graphene quantum dots. Unlike those synthesized through stepwise carbon–carbon bond formation by organic reactions (bottom-up method), NGs obtained by cutting parent carbons (top-down method) pose challenges in precisely regulating their three-dimensional structures by post-synthesis. This includes the incorporation of non-hexagonal rings and helicene-like structures in carbon frameworks. Currently, edge functionalization is the only method for generating chirality in NGs produced by the top-down method. While various chiral NGs have been synthesized through organic methods, examples of chemical modification remain rare due to limited structural information and the substantial size of NGs. However, these problems can be mitigated by disclosing the structures of NGs, particularly their edge structures. This mini-review focuses on recently published papers that have addressed the structural characterization of NGs and their chirality generation by edge modification. Comparing these NGs with those synthesized by organic synthesis will help to develop reasonable strategies for creating sophisticated chiral NGs. We hope this mini-review contributes to the advancement of NG–organic hybrid materials.

Received 16th July 2024,
Accepted 15th November 2024

DOI: 10.1039/d4nr02952f

rsc.li/nanoscale

Introduction

Chirality significantly impacts homochirality. A molecule becomes chiral when it lacks an improper axis of symmetry, such as a plane of symmetry or a center of inversion. Helically curved polycyclic aromatic hydrocarbons (PAHs), known as helicenes,[1] exhibit exceptional chiroptical properties compared to their linear counterparts. Recently, chiral nonplanar PAHs, also known as chiral nanocarbons or chiral nanographenes (NGs), have become a significant area of study in synthetic organic chemistry. Researchers have developed a diverse range of nonplanar chiral NGs through manipulating their three-dimensional structures by incorporation of helicene-like frameworks and/or non-hexagonal rings.

These NGs were synthesized through stepwise carbon–carbon bond formation and aromatization (bottom-up method). However, the production of NGs is not limited to organic synthesis. NGs can also be obtained through the cleavage of parent carbons, such as graphite and carbon fibers (top-down method). These NGs typically have diameters ranging from a few to tens of nanometers and can be considered graphene fragments.[2,3] Although these NGs are mixtures of various sizes and shapes, their gram-scale production within a few reaction steps is attractive for developing NG–organic hybrid materials. During the oxidative cleavage of the parent carbons, oxygen-containing functional groups, such as carboxy and hydroxy groups, are generated on the edges, enabling the chemical modification of NGs (Fig. 1).[4–13] For example, the installation of naphthalene-1,8-diamine derivatives into the edges, allowed by covalent linkages between the edge and the installed small aromatic systems, facilitates electronic interactions between them.[14] This connection of the two π systems influences their optical properties, resulting in

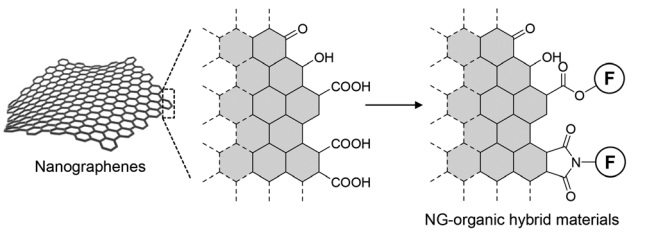

Fig. 1 Edge functionalization to realize NG–organic hybrid materials.

[a]*Department of Chemistry, Graduate School of Advanced Science and Engineering, Hiroshima University, 1-3-1 Kagamiyama, Higashi-Hiroshima, Hiroshima, 739-8526, Japan*
[b]*Department of Frontier Materials Chemistry, Graduate School of Science and Technology, Hirosaki University, 3 Bunkyo-cho, Hirosaki, Aomori, 036-8561, Japan. E-mail: csekiya@hirosaki-u.ac.jp*
[c]*International Institute for Sustainability with Knotted Chiral Matter (SKCM²), Hiroshima University, 1-3-1 Kagamiyama, Higashi-Hiroshima, Hiroshima, 739-8526, Japan. E-mail: haino@hiroshima-u.ac.jp*

photoluminescence (PL) in the near-infrared region. Edge functionalization with triphenylamines has offered electrochromic materials functioning in the near-infrared region.[8] Recently, our group[6,9] and Martín's group[15] independently reported the controlled self-assembly of NGs. These examples demonstrated the potential of NGs in creating functional carbon materials.[4]

A remaining and underdeveloped topic is the generation of chirality in NGs through chemical modification. The combination of chirality and PL properties of NGs could yield excellent chiroptical properties, comparable to those produced by organic synthesis. However, chiral NGs synthesized by chemical modification are rare compared to those produced by organic synthesis. This scarcity is partly due to limited structural information on NGs, as they are composed of a nonstoichiometric mixture of graphene fragments of various sizes and shapes, and their structures are not fully disclosed. This lack of detailed structural information complicates the development of effective strategies for generating chirality in NGs. Additionally, the large surface area of NGs with diameters ranging from a few to tens of nanometers makes it challenging to rigidify and amplify the induced chirality. While the latter issue persists with top-down method-based NGs, the former can be mitigated by disclosing NG structures, particularly their edge structures. Hence, information from recent studies on the structural characterization of NGs and their chirality generation is crucial.

Based on this background, this mini-review is structured as follows: we first provide three representative production methods for NGs. We then focus on the generation of structures and chirality, discussing computational approaches that address the structural characterization of NGs. This information is valuable for developing effective strategies to create sophisticated chiral NGs. We hope this mini-review will contribute to advancing the field of NG–organic hybrid materials.

Discussions

Production methods can be categorized into bottom-up and top-down methods (Fig. 2). Bottom-up methods are further subdivided into organic synthesis and graphitization. As the NGs produced by these methods have distinct structures, their chirality generation strategies completely differ from each other. Briefly, the bottom-up methods embed chirality in carbon frameworks to realize chiral NGs, while the top-down method installs chiral sources into the edge of NGs to generate chirality on NGs.

Organic synthesis

Organic synthesis involves constructing carbon frameworks through organic reactions. Stepwise carbon–carbon bond formation and cyclodehydrogenation with suitable oxidants, such as those through Pd-catalyzed cross-coupling and Scholl reactions, produce NGs. Fig. 3a shows a typical example of an NG produced by organic synthesis.[16] The formation of carbon–carbon bonds and aromatization with 2,3-dichloro-5,6-dicyano-1,4-benzoquinone yielded helically twisted NGs.

Well-defined carbon frameworks allow for an in-depth analysis of their physical properties using spectroscopic methods, such as ^{1}H- and ^{13}C{^{1}H}-nuclear magnetic resonance (NMR) spectroscopy, and absorption, circular dichroism (CD), and PL

Ryo Sekiya

Ryo Sekiya graduated from Sophia University in 1998 and received his Ph.D. degree from the University of Tokyo in 2003. He then moved to Chiba University as a JSPS young researcher. In 2004, he was appointed assistant professor at the Graduate School of Arts and Sciences, University of Tokyo. In 2012, he joined the group of Professor Takeharu Haino at Hiroshima University as an associate professor. In 2016, he joined the group of Pablo Ballester at the Institutes Català d'Investigació Química in Spain and was appointed as a visiting professor at Orenburg State University in the Russian Federation. In 2024, he was appointed a full professor in the Department of Frontier Materials Chemistry, Graduate School of Science and Technology, Hirosaki University. His research interests are supramolecular chemistry, solid-state organic/inorganic chemistry, and graphenes.

Saki Arimura

Saki Arimura received her B.Sc. in chemistry from Hiroshima University in 2022 and her M.Sc. in chemistry in 2024. She is now working as a researcher in a company. Her research interest is functionalized carbon materials.

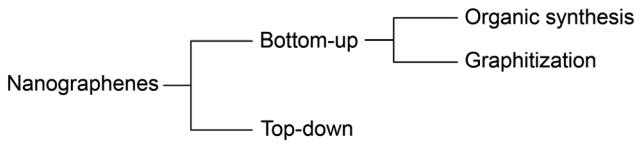

Fig. 2 Classification of NG production methodologies: organic synthesis, graphitization, and top-down method.

spectroscopy. Cyclic voltammetry also offers valuable information. Furthermore, these chiral NGs can yield single crystals, enabling single-crystal X-ray diffraction analysis. This analysis can reveal three-dimensional structures of NGs with angstrom-level accuracy. Computational approaches are also useful for assessing electronic structures.

Non-planar PAHs can be achieved by incorporating non-hexagonal ring(s) and/or helicene-like structure(s) into their carbon frameworks.[21,22] A five- or four-membered ring can induce a positive curvature, whereas a seven- or eight-membered ring can induce a negative curvature in the carbon framework. The structures with the former curvature include fullerenes and corannulenes, while the latter curvature results in saddle-shaped carbon frameworks. Combining non-six-membered rings and helicene-like frameworks has led to numerous nonplanar chiral NGs.[16–20,23–34] Due to limited space, only a few nonplanar chiral NGs reported in 2020–23 are briefly introduced in the following section.

Campaña *et al.* reported interesting chiral saddle–helix hybrid NGs (Fig. 3b-i),[17] containing a nine-membered ring at their periphery, resulting in a sizeable interplanar angle (134.8°). Due to the rigidification of the carbon framework by the nonagonal ring, these NGs showed excellent tolerance for racemization. The same group also reported octagon-embedded NGs,[26] which, like nonagonal-ring-embedded NGs, exhibited a significant twist in the carbon framework. A negatively curved NG containing a heptagon ring was reported by Müllen and Narita *et al.* (Fig. 3b-ii).[18] The combination of the five- and eight-membered rings resulted in unique carbon frameworks. For instance, Mastalerz *et al.* reported monkey saddle-like NGs by embedding five- and eight-membered rings surrounding a central benzene ring in an alternate fashion (Fig. 3b-iii).[28] In addition to these non-hexagonal ring-containing NGs, fully hexagonal chiral NGs have also been actively constructed. Gong *et al.* realized four hexabenzocoronene-fused helical NGs.[23] Coquerel *et al.* developed NGs with three helicene units (Fig. 3b-iv).[20]

An important feature of chiral NGs is their chiroptical properties. Fig. 4 shows the molecular structures of three chiral NGs (NGG, NGB, and NGR) and their absorption (solid line) and PL (dashed line) spectra, as well as the CD and circularly polarized luminescence (CPL) spectra of NGR and NGG in dichloromethane as reported by Campaña *et al.*[26] The structurally rigid carbon frameworks allowed for optical resolution by HPLC. The resulting homochiral NGs exhibited well-resolved CD (250–450 nm) and CPL spectra (450–700 nm).

As demonstrated by Campaña *et al.*, the structural rigidity of carbon frameworks is crucial for realizing excellent chiroptical properties. To achieve optical resolution, sufficient activation energy is required to suppress racemization at room temperature. Martín *et al.* categorized chiral NGs into four classes according to the energy barrier of chiral inversion:[35] flexible (<5 kcal mol^{-1}), detectable (5–20 kcal mol^{-1}), isolable (20–35 kcal mol^{-1}), and rigid (>35 kcal mol^{-1}) (Fig. 5). These chiral NGs are classified as isolable or rigid NGs. Martín

Haruka Moriguchi

Haruka Moriguchi received his B.Sc. in chemistry from Hiroshima University in 2023. He is now in the second year of his master's program. His research interest is controlling the assembly of nanographenes and the function of the assembled nanographenes.

Takeharu Haino

Takeharu Haino received his Ph.D. degree from Hiroshima University in 1992. He then moved to Sagami Chemical Research Center. In 1993, he was appointed assistant professor in the Department of Chemistry at Hiroshima University. He joined the group of Professor Julius Rebek, Jr. at The Scripps Research Institute (1999–2000). He was promoted to associate professor in 2000, to full professor in 2007, and to distinguished professor in 2021. He is also a principal investigator at the International Institute for Sustainability with Knotted Chiral Meta Matter (WPI-SKCM^2). He has served as an associate editor of the Bulletin of the Chemical Society of Japan. *His research interests are in the developments of functional graphene materials, supramolecular polymers, chiroptically active assemblies, and supramolecular catalysts.*

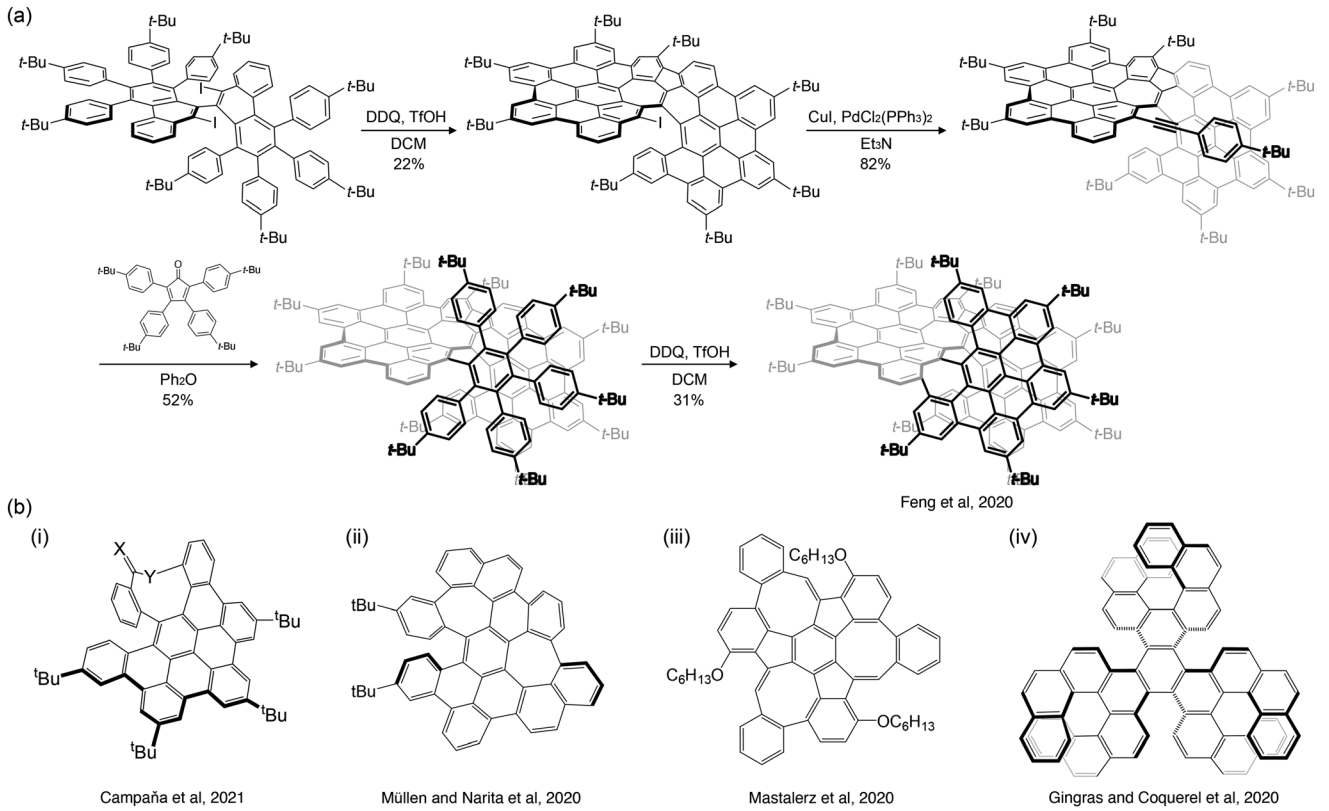

Fig. 3 (a) Example of the synthesis of NG by organic synthesis (ref. 16). (b) Non-planar chiral NGs synthesized by organic synthesis as reported by (i) Campaña *et al.* (ref. 17), (ii) Müllen and Narita *et al.* (ref. 18), (iii) Mastalerz *et al.* (ref. 28), and (iv) Gingras and Coquerel *et al.* (ref. 20).

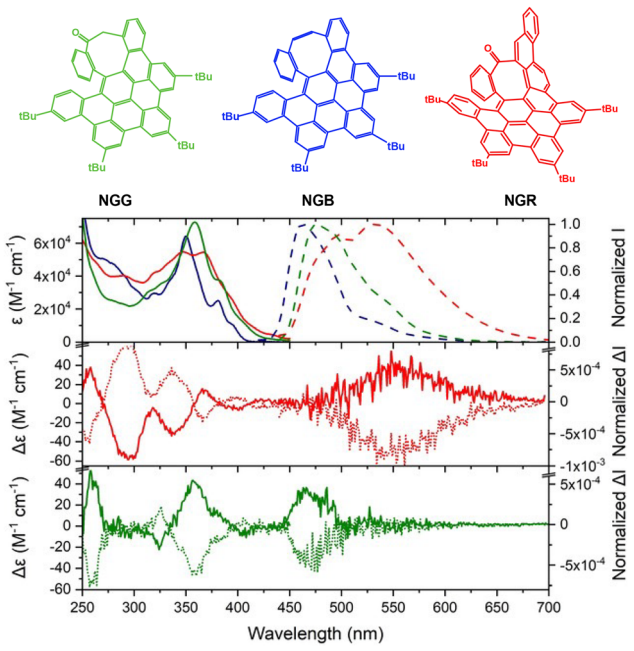

Fig. 4 Molecular structures of NGG, NGB, and NGR. (Top) UV-vis absorption and PL spectra of NGG (green), NGB (blue), and NGR (red) in dichloromethane. (Middle and bottom) ECD (250–450 nm) and CPL (450–700 nm) spectra of (middle) NGR and (bottom) NGG in dichloromethane (ref. 26). Copyright 2021, Wiley-VCH.

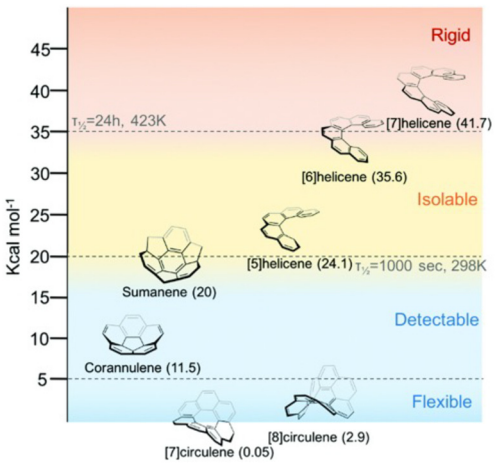

Fig. 5 Classification of NGs based on the energy barrier (ref. 35). Copyright 2022, Royal Society of Chemistry.

et al.'s classification is helpful for assessing the current stages of chiral NGs realized by edge modification.

Graphitization

Although graphitization also employs small molecules as carbon sources, the procedures differ completely from organic

synthesis. A typical method is the solvothermal reaction of small organic molecules. Under high temperatures and high-pressure conditions, organic molecules decompose and reorganize to produce graphitic materials. A well-known example is the graphitization of citric acid.[36] Chi *et al.* reported that the heating of citric acid at 200 °C for 30 min produces NGs. Prolonged heating resulted in large graphitic sheets, indicating that the basal planes gradually grew during the reaction.

Graphitization inevitably produces a mixture of NGs of distinct sizes and shapes, as demonstrated by Chi *et al.* These NGs, or more precisely, mixtures of NGs, often display excitation wavelength-dependent PL. Experimental and theoretical approaches have been devoted to explaining this phenomenon, such as the PL from isolated aromatic areas (sp^2 domains).[37] Lim and Chen *et al.* computed sp^2 domains surrounded by sp^3 carbons and suggested that these domains are responsible for the excitation-wavelength-dependent PL.[37] Urban *et al.* supported the latter hypothesis based on the PL spectra of PAH mixtures.[38] Column chromatographic separation of NGs further supported the latter hypothesis; the size separation of nitrogen-doped NGs yielded size-separated NGs emitting various colors.[39] Excitation-wavelength-dependent PL properties of NGs can be found in other studies.[40,41]

Because the physical properties of NGs, such as those producing their PL spectra, can be influenced by their size distribution, controlling the size or narrowing the size distribution of NGs is crucial for enhancing the reproducibility of these physical properties. Müllen *et al.*[42] provided an excellent example by demonstrating the synthesis of mono-dispersed disk-like NGs with ~60 nm diameter and 2–3 nm thickness through the pyrolysis of hexa-*peri*-hexabenzocoronene aggregates followed by oxidative cleavage, functionalization, and reduction with hydrazine.

Graphitization offers the advantage of utilizing various organic molecules as carbon sources. When these carbon sources contain heteroatom(s), such as boron,[43] nitrogen,[39,44,45] sulfur,[46] and phosphorous,[47] heteroatom-doped NGs can be produced (Fig. 6a).[48] The presence of these heteroatoms, with their three (B), five (N, P), and six (S) valence electrons, can modify the electronic structures of the carbon framework. For instance, nitrogen-doped NGs were synthesized from *o*-, *m*-, and *p*-phenylenediamine *via* solvothermal reactions (Fig. 6b),[44] each showing distinct optical properties. Nachtigallová and Zbořil *et al.*,[39] similarly employed citric acid and urea as carbon sources in formamide, resulting in NGs emitting blue, green, yellow, and red light after separation on a preparative anion-exchange column (Fig. 6c). The emission color was influenced by the nitrogen content and its positioning within the carbon framework, as suggested by time-dependent density functional theory (TD-DFT) calculations that indicated narrowing of the HOMO–LUMO gap by nitrogen atoms.

Given the versatility of graphitization in utilizing diverse organic molecules as starting materials, researchers have explored employing chiral molecules to produce chiral NGs. Despite the limited number of examples for producing chiral NGs by graphitization,[49] Đorđević and Prato *et al.* reported the

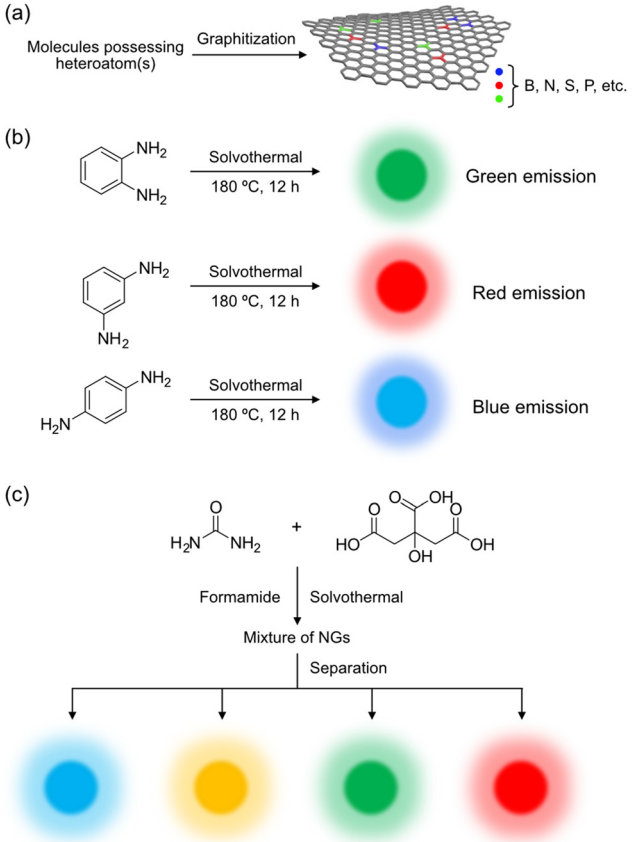

Fig. 6 (a) Schematic illustration of a hetero-atom-doped NG. (b) Production of NGs by graphitization of *o*-, *m*-, and *p*-phenylenediamines under solvothermal reaction conditions. The resultant NGs emitted green, red, and blue light. (c) Solvothermal reactions of citric acid and urea in formamide. Column chromatographic separation of as-produced NGs with anion-exchange column offers NGs emitting blue, green, yellow, and red light. In (b) and (c), the nitrogen content and location of the nitrogen atoms in the carbon frameworks influence the color of light by regulating the HOMO–LUMO gap.

microwave-assisted hydrothermal synthesis of chiral carbon nanodots, which are generally considered carbon nanoparticles with carbon cores covered by oxygen-containing functional groups,[49] from (*R*,*R*)- or (*S*,*S*)-cyclohexane diamine and arginine (Fig. 7), yielding products with mirrored CD spectra. This preservation of chirality from the starting chiral sources after graphitization suggests that chiral information may persist in ungraphitized areas (*e.g.*, sp^3 carbons) of the carbon frameworks and/or on the edge, even as graphitization primarily produces sp^2 carbons and diminishes chirality.

Although graphitization is appealing for its straightforwardness and, therefore, is an attractive method, ensuring the purity of the products is essential. When unreacted starting materials and/or chiral byproducts coexist with the products, the observed CD and CPL spectra can be contaminated by chiral molecular species. This contamination should be removed from products, especially when the coexisting chiral molecular species have high molar extinction coefficients and/or PL quantum yields. Prato *et al.* reported this possibility in

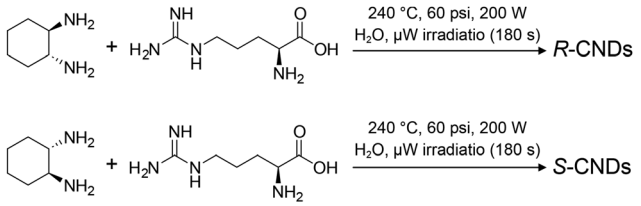

Fig. 7 Chiral carbon nanodots (CNDs) synthesized from (*R,R*)- and (*S,S*)-1,2-cyclohexane diamine and arginine under microwave-assisted hydrothermal synthesis (ref. 49).

three case studies.[50] They demonstrated that the observed CD spectra did not originate from NGs but from coexisting starting materials or byproducts. They suggested that the ^{1}H-NMR spectroscopy could effectively verify the purity of the products. Coexisting molecular species (starting materials and byproducts) show sharp signals, whereas graphitized species show broad signals.

Oxidative cleavage

The top-down method offers NGs through the cleavage of carbon sources,[41] such as graphite,[13] graphene obtained by thermal deoxidation of GOs, fullerene,[52] and carbon nanofibers.[53] Fig. 8a shows an example of the production of NGs by acid-assisted oxidative cleavage of graphite developed by our group. Neutralization followed by deionization with dialysis membranes (pore size: 2 kDa) and acidification with acid chloride provides carboxy-group-terminated NGs, which can be used as starting materials for NG–organic hybrid materials.[51]

One advantage of this protocol is the production of NGs with minimally oxidized surfaces. ^{13}C{^{1}H}-NMR spectra of the NGs in D_2O showed no signals assignable to oxidized sp^3 carbons. This contrasts sharply with GOs produced by modified Hummers methods.[54] Solid-state CP/MAS NMR spectra of ^{13}C-enriched GOs showed strong peaks assignable to oxidized sp^3 carbons.[55] A possible explanation for the lack of signals in oxidized carbons is that surface oxidation does not occur randomly but linearly. A theoretical calculation of the unzipping of GOs suggests that the strain generated by the cooperative alignment of epoxy groups can initiate cracks in GOs.[56] This calculation provides insight into the mechanism of oxidative cleavage. When oxidation occurs linearly on the surface, the cleavage of the oxidized parts leaves NGs with minimally oxidized surfaces.

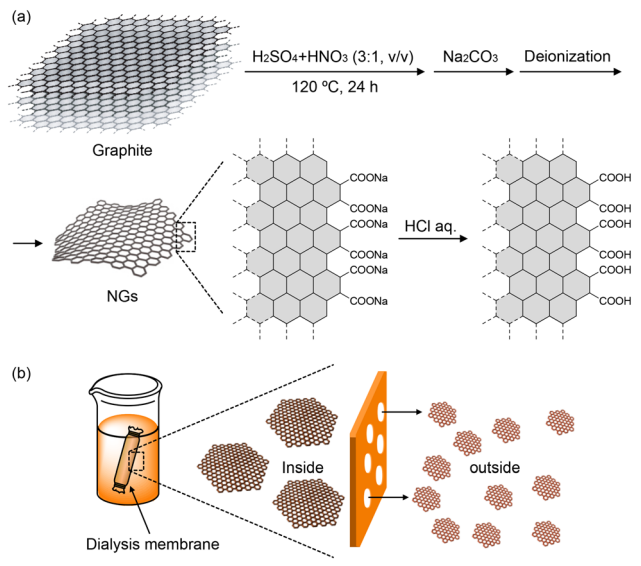

Fig. 8 (a) Production of NGs by oxidative cleavage of graphite with a mixture of nitric acid and sulfuric acid. Note: the surfaces of NGs are drawn with single lines. (b) Size separation of NGs with dialysis membranes (ref. 51).

Similar to graphitization, the top-down method produces NGs as mixtures of various sizes and shapes. Several groups have conducted size separation of NGs. Matsuda *et al.* reported the size separation of as-produced NGs by HPLC.[57] Guo and Zhang *et al.* separated NGs by gel electrophoresis.[58] Our group conducted the size separation of edge-functionalized NGs by size-exclusion chromatography.[59] A convenient and inexpensive procedure is the utilization of dialysis membranes, which allows gram-scale size separation of NGs (Fig. 8b).[51,60] When dialysis membranes with a pore size of 50 kDa are used, NGs smaller than the pores leak out, while those larger than the pore size remain inside. Repeated utilization of dialysis membranes with distinct pore sizes offers separation of NGs with a narrow size distribution; however, this procedure is time-consuming and needs improvement. Furthermore, because this protocol relies on the pores in the dialysis membranes, the accuracy of size separation is inevitably inferior to that of HPLC.

The structure of NGs depends on the carbon source and production method. For example, Ajayan *et al.* suggested that NGs produced from carbon fibers have carbonyl-terminated zigzag edges (Fig. 9a).[53] We showed that acid-assisted oxidative cleavage of graphite yields NGs with the carboxy group-terminated armchair edge as the dominant edge structure (Fig. 9b).[13] Subsequently, we reported that distinct carbon sources (graphite, finely crushed graphite powders, and artificial graphite) provided NGs with similar edge structures, although their optical properties differed slightly.[60] The characterization of our examples was based on comparing IR spectra.

Characterization of edges is crucial because their structure and the existing functional groups on the edge determine the procedures for edge modification. The reaction of carboxy-terminated edges with organic amines yielded three types of structures. The isolated carboxyl groups on the zigzag and armchair edges provide amides. When two carboxyl groups are arranged along the zigzag edge, amides and/or six-membered imides are formed (Fig. 9c). The two carboxyl groups on the armchair edge provide five-membered imides. Although it is difficult to distinguish between amides and five- and six-membered imides using ^{13}C{^{1}H}-NMR spectroscopy, IR spectroscopy can be used. The amides exhibited both C=O and N–H stretching vibrations. In contrast, the six- and five-mem-

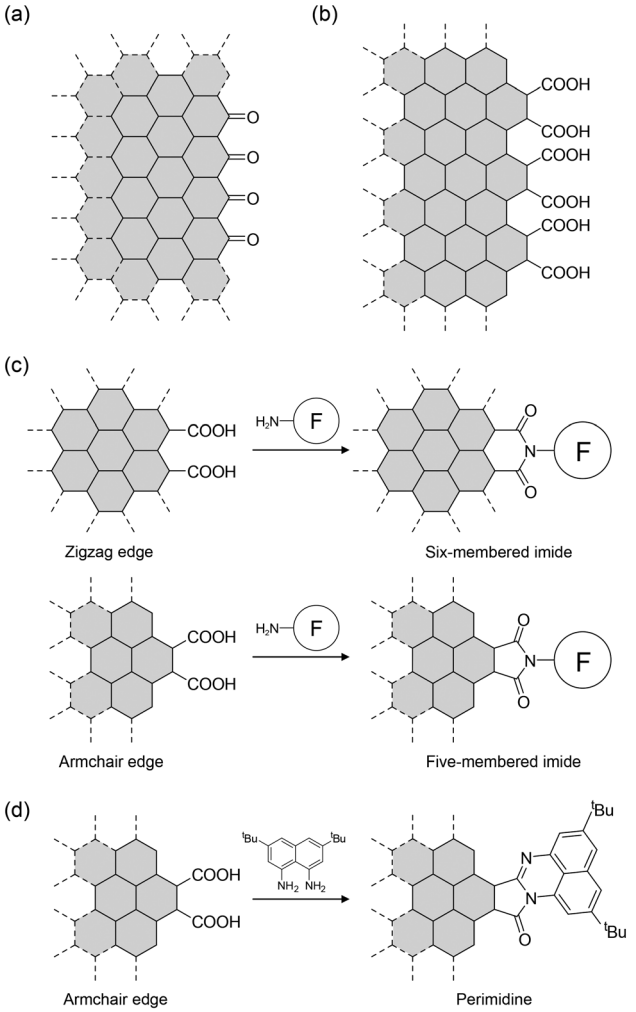

Fig. 9 Proposed edge structures of NGs produced from (a) carbon fiber and (b) graphite. (c) Possible edge structures and their edge modifications with organic amines. The zigzag edge gives a six-membered imide ring on the zigzag edge, while the armchair edge gives a five-membered ring on the armchair edge. (d) Condensation of the armchair edge with 3,6-di(*tert*-butyl)naphthalene-1,8-diamine.

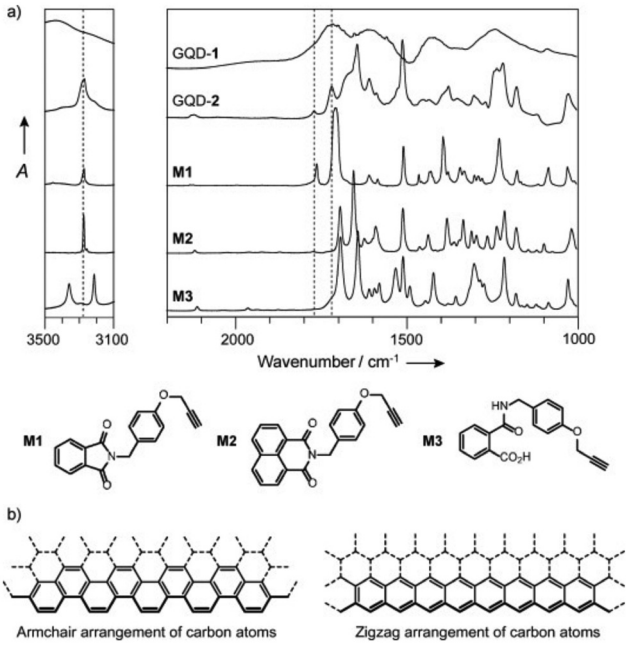

Fig. 10 (a) IR spectra of NG (GQD-**1**), edge-functionalized NG (GQD-**2**), and model compounds (**M1**–**M3**). (b) Armchair (left) and zigzag (right) edges of NGs (ref. 13). Copyright 2014, Wiley-VCH.

bered imides show weak and strong pairs of C=O stretching vibrations caused by symmetric and asymmetric vibrations, respectively, and no N–H stretching vibrations. Because the ring size of the imide influences the wavenumbers of the C=O stretching vibrations,[61] six- and five-membered imides are distinguishable using IR spectroscopy.

A more reliable characterization method is to compare the IR spectra of functionalized NGs with those of structurally known model compounds. One example is shown in Fig. 10.[63] The comparison of the observed IR spectrum of functionalized NGs (GQD-**2** in Fig. 10a) with those of model compounds (**M1**–**M3** in Fig. 10a) demonstrated that the two C=O stretching vibrations of the functionalized NGs were in good agreement with those of **M1** which has a five-membered imide. Hence, the dominant edge structure was an armchair edge with two carboxyl groups. Comparing the spectroscopic data of functionalized NGs with those of structurally known model compounds can be widely utilized to characterize the edge structures of graphitic materials, including NGs produced by graphitization. This edge structure was supported by the reaction of NGs with 1,8-naphthalene diamine derivatives, which produced perimidine at the edges (Fig. 9d).[14]

The above observations, specifically the presence of an armchair edge with two carboxyl groups on the edge, provide a rough image of the NG edge structures. Fig. 11a shows a model NG composed of 174 carbon atoms, which was designed based upon experimental observations.[62] Although the size of the model NG is much smaller than the actual NGs, DFT calculations provided valuable information. The calculations predict an up-and-down puckered edge. The flat structure of the core originates from the fully hexagonal rings in the carbon framework. The puckered edge results from the steric contact between neighboring carboxy groups. The puckered structure is predicted to be retained after the edge functionalization (Fig. 11c). Hence, regulating edge distortion is the first step in realizing chiral NGs through chemical modification.

The installed functional groups can adopt various orientations at the edges. A computational study predicted that up-and-down and twisted orientations were possible orientations of the five-membered imides on the edge (Fig. 12a).[64] A model of the edge extracted from a NG with *N*-methyl five-membered imides predicted twisted surfaces when the functional groups pointed in distinct directions (up-and-down orientation) or when the functional groups were twisted relative to the edge (twisted orientation) (Fig. 12b and c).

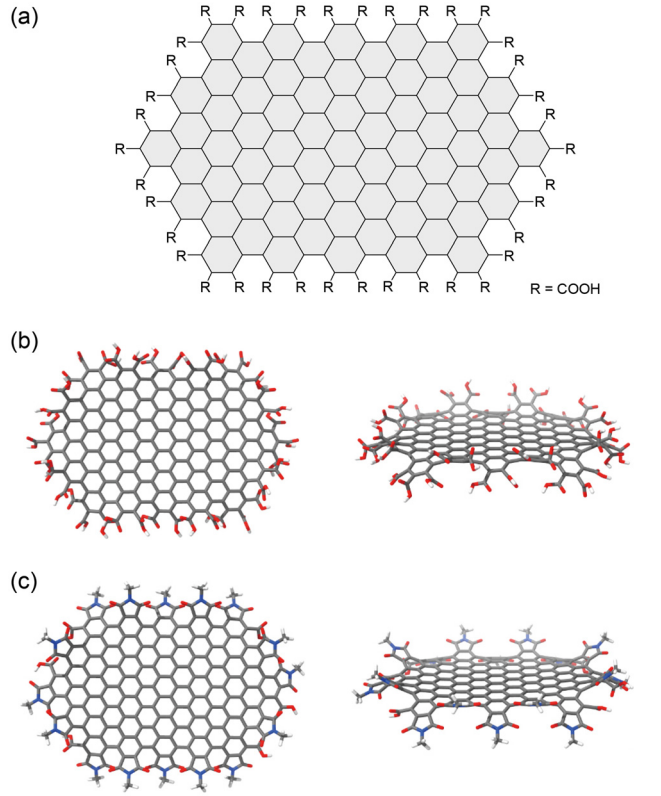

Fig. 11 (a) Chemical structure of a model NG used for the DFT calculation. Optimized structures of (b) carboxy-terminated and (c) *N*-methyl cyclic imide-terminated model NGs at the B3LYP/6-31G(d,p) level of functionality. Color scheme: gray (carbon), white (hydrogen), blue (nitrogen), red (oxygen) (ref. 62). Copyright 2023, Wiley-VCH.

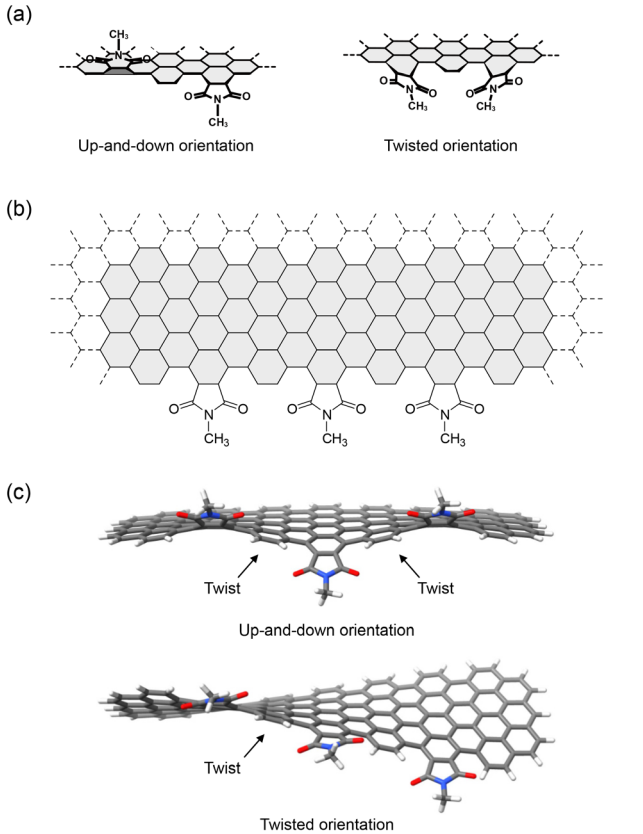

Fig. 12 (a) Up-and-down (left) and twisted orientations (right). (b) Chemical structure of the model edge used for the DFT calculations. (c) Optimized structures of the model edge carrying *N*-methyl five-membered imides on the edge. Color scheme: gray (carbon), white (hydrogen), blue (nitrogen), red (oxygen) (ref. 5). Copyright 2023, Wiley-VCH.

Because this NG has a vast surface area and a long annular edge, twists are likely to be generated at various sites on the edge. Thus, one strategy for chirality generation is to bias the twist direction by installing chiral functional groups and rigidifying and amplifying the induced chirality. Chirality information is conveyed from the installed chiral source to the NGs through steric contacts and/or intermolecular interactions, such as π–π stacking interactions (Fig. 13a). These contacts and/or interactions can bias the direction of twisting. The following section introduces chiral NGs produced by the chemical modification of NGs.

The earliest example was reported by Kotov *et al.* in 2016.[65] They conducted edge functionalization with D- and L-cysteine (Fig. 13b-i). CD spectra and computational calculations indicate the generation of left- and right-handed helicity on the basal plane. Non-covalent interactions between the installed D- and L-cysteine and the edge are likely to bias the twist direction, resulting in chiral NGs. A similar procedure was reported by Martín *et al.* in 2016 (Fig. 13b-ii).[66] Interestingly, they reported that the aggregation of chiral NGs carrying (*R*)- or (*S*)-phenylethyl alcohol and pyrene conveyed chirality from NGs to pyrene, allowing for the CPL emission of pyrene. Subsequently, the same group reported an interesting protocol for chirality transfer. They installed pyrene-terminated chiral functional groups at the edge (Fig. 13b-iii), and the π–π stacking interaction between the pyrene unit and the surface secured chirality transfer.

Our group has also contributed to the development of chiral NGs.[10] (*R*)- and (*S*)-phenylethylamines and (*R*)- and (*S*)-*p*-bromophenylethylamine were installed at the edges to realize chiral NGs (NGH and NGBr in Fig. 13b-iv). The CD spectra of (*R*)- and (*S*)-NGH (Fig. 14a) were similar in shape to those of the model compounds. More concentrated solutions showed weak CD signals over 350 nm, indicating chiral transfer from the chiral functional groups to the NGs. In the case of (*R*)- and (*S*)-NGBr, complex CD spectra were observed (Fig. 14b), caused by exciton coupling[67–69] between neighboring chiral functional groups on the edge. This suggests that the functional groups on the edges are close enough to interact with each other.

The X-ray crystal structure analysis of a model compound provided clues for chirality transfer (Fig. 15a).[10] The contact between the methyl group on the stereogenic center and the carboxyl group on the phthalimide induced a twist of approximately 2° between the benzene ring and the five-membered imide ring. This suggests that steric contacts between the methyl group on the stereogenic center, the carbonyl group on

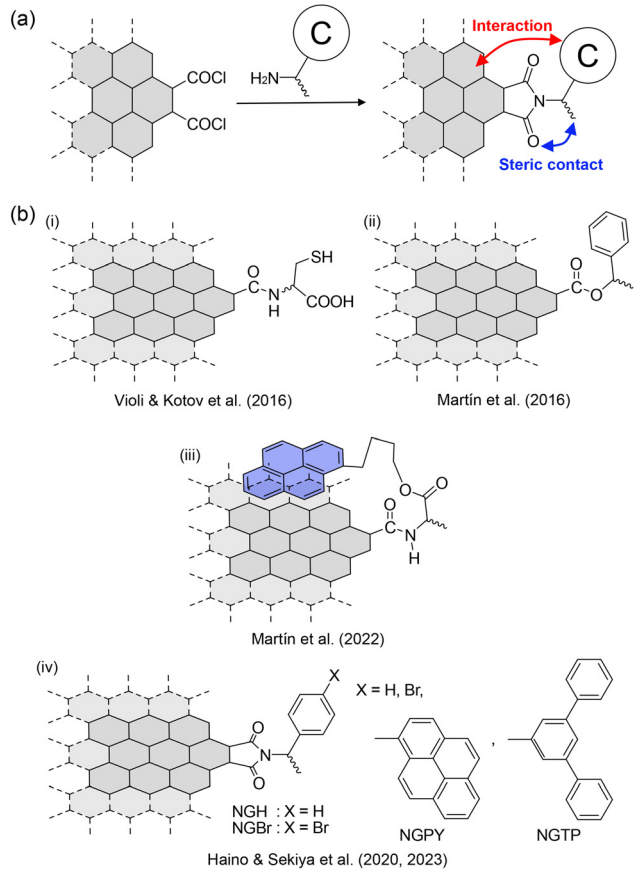

Fig. 13 (a) Strategy of edge functionalization of NGs produced by the top-down method. (b) Examples of chirality generation on NGs by the edge functionalization reported by (i) Violi and Kotov *et al.* (ref. 65), (ii) and (iii) Martín *et al.* (ref. 66 and 15), (iv) Haino and Sekiya *et al.* (ref. 10 and 5).

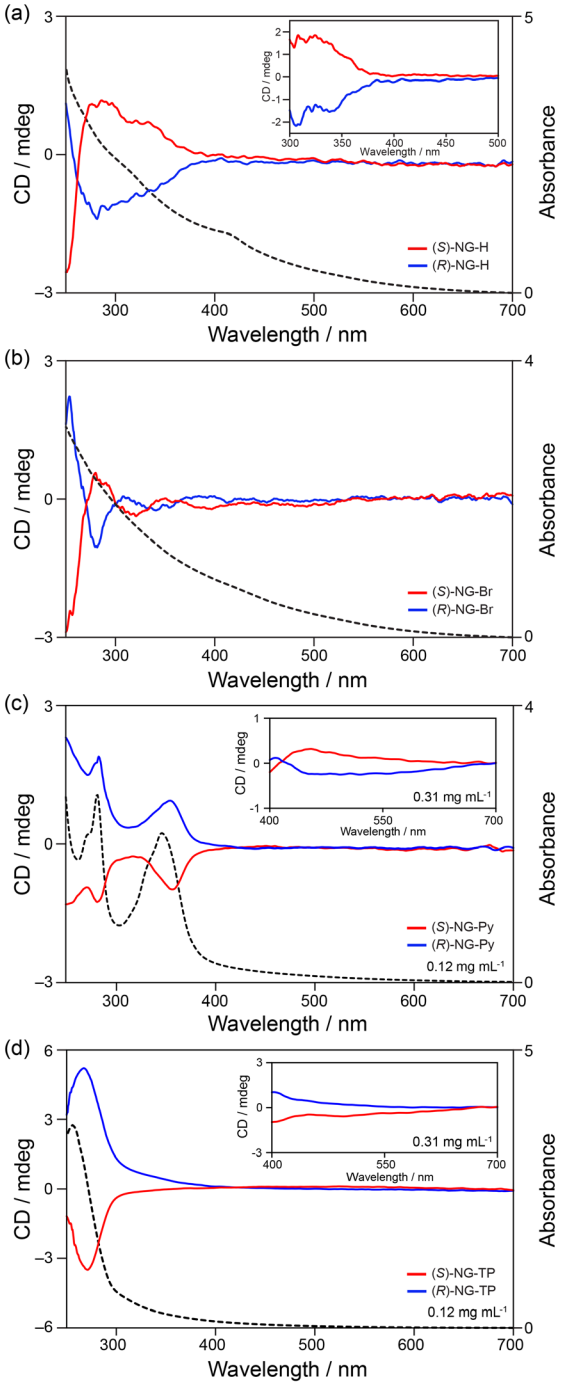

Fig. 14 Observed CD spectra of (a) NG-H, (b) NG-Br, (c) NG-pyrene, and (d) NG-terphenyl in chloroform (ref. 10 and 5). Red lines represent the (*R*)-enantiomers and blue lines represent the (*S*)-enantiomers. Black dotted lines are the UV-vis absorption spectra of the (*S*)-enantiomers. Copyright 2020 & 2023, Wiley-VCH.

the imide, and the edge are routes for chirality transfer (Fig. 15b).

Compared to chiral NGs synthesized by organic methods, the above examples show very weak CD spectra, and their CD spectra are not perfect mirror images. One possible explanation for the former is that the steric contacts and/or intermolecular interactions between NG and the chiral functional group are insufficient to rigidify the induced chirality, resulting in a slight twist bias on the edge. This is because the installed functional groups protrude from the edge and the rotatable C–N single bond connects the functional groups and NGs. Imperfect mirror-image CD spectra may arise from the nonstoichiometric mixture of these chiral NGs. Based on the classification by Martín *et al.* (Fig. 5), these NGs can be categorized as flexible to detectable, although the energy barriers of chirality inversion are difficult to estimate. Hence, the generation of chirality in NGs by chemical functionalization is still in the early stages of development.

Steric contacts between the functional groups and edges can rigidify the induced chirality. This can be achieved by installing bulky chiral functional groups on the edges. Bulky substituents would also hinder the rotation of C–N single bonds through steric contact between them. This strategy is supported by the edge modification of NGs with bulky and less bulky substituents (Fig. 16),[12] although this example involves non-chiral NGs. NGs carrying third-generation dendri-

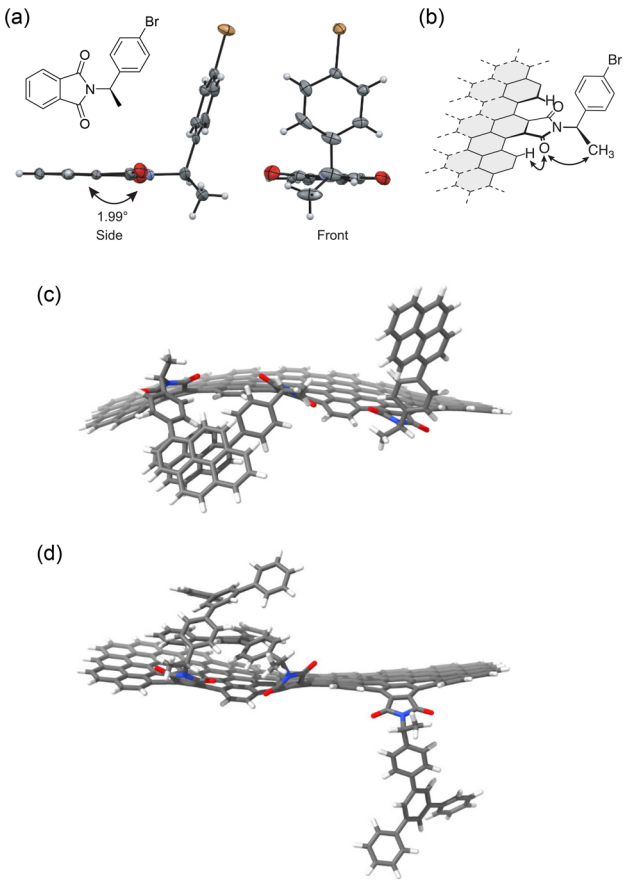

Fig. 15 X-ray crystal structure of a model compound carrying an (*R*)-*p*-bromophenylethyl group. (b) Possible mechanism of chirality transfer from the stereogenic center to the edge of the NG (ref. 10). (c) and (d) Optimized structures of the model edges of NGPY and NGTP (ref. 5). In (a), (c), and (d) Color scheme: gray (carbon), white (hydrogen), blue (nitrogen), red (oxygen), brown (bromine). Copyright 2020 & 2023, Wiley-VCH.

tic wedges had smaller effective conjugated areas than those with less bulky substituents. One reason is that the effective π conjugation was narrowed to avoid steric contact between neighboring dendritic wedges.

Recently, an example was reported[70] where the bromine atoms on NGBr were substituted with pyrene (NGPY) and *p*-terphenyl (NGTP) through Pd-catalyzed cross-coupling reactions. The CD spectra of (*R*)- and (*S*)-NGPY and NGTP showed improved CD signals (Fig. 14c and d). CD signals were observed in the visible region, although the signal intensities were weak. Interestingly, the CD signals of (*R*)- and (*S*)-NGPY and NGTP were opposite to each other, likely due to the induction of opposite chirality despite having the same absolute configuration on the stereogenic centers. DFT calculations suggested that the pyrene and *p*-terphenyl groups interacted with the surface through π–π stacking interactions (Fig. 15c and d). The interactions between the surface and the pyrene groups and those between the surface and the *p*-terphenyl groups may differ, resulting in an opposite twist on the edge.

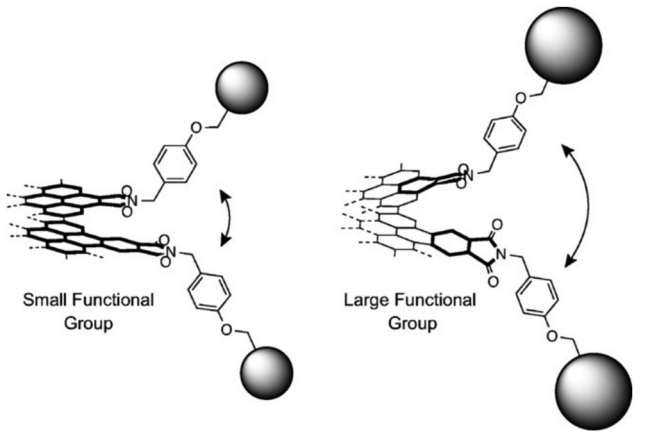

Fig. 16 Schematic representation of (left) small and (right) large substituents on the edge. The latter may cause a larger twist on the edge (ref. 12). Copyright 2016, Wiley-VCH.

These observations indicate that not only the chirality of the stereogenic centers but also the interactions between the functional group and the surface and/or neighboring functional groups on the edge can influence the chirality of NGs.

Advantages and disadvantages

We briefly summarize the advantages and disadvantages of the three methods for developing chiral NGs. The advantage of the bottom-up method by organic synthesis is undoubtedly structurally well-defined carbon frameworks. Their structures and functions, such as optical properties and chirality, can be tuned precisely. A disadvantage might be a multi-step synthesis to construct carbon frameworks, although this is not severe. An advantage of the bottom-up method by graphitization is that various chiral sources can be used as starting materials. However, the contamination of starting materials and/or byproducts can lead to wrong conclusions. Also, the characterization, for example, where chiral sources exist and how chirality is generated on NGs, would be troublesome. Hence, this method may suffer from the tunability of functions. By contrast, the top-down method can tune their functions by edge modification. The gram-scale production of NGs is also attractive from the perspective of practical applications. However, the non-stoichiometry of NGs can be troublesome. Further, we must overcome inefficient chirality transfer and rigidify the induced chirality on the surface by developing sophisticated chiral functional groups.

Chirality and structural analysis

This section presents a structural analysis of NGs based on chirality. A recent method to analyze the edge structures of NGs was reported.[71]

Exciton coupling was used to determine the absolute configurations of chiral molecules. This coupling occurs when chiral chromophores are in close proximity.[69] The exciton coupling is defined as $R_{ij}(\mu_{i0a} \times \mu_{j0a})\cdot V_{ij}$, where R_{ij} is an interchromophoric distance vector from chromophores i to j, μ_{i0a}

and μ_{j0a} are the electronic transition moments of chromophores i and j from the ground state to the excited state a, and V_{ij} is the interaction energy. When two chromophores approach the edge at a certain distance, the spectral shape changes (Fig. 17a). For example, *p*-bromo- and *p*-methoxy benzoate chromophores on a cyclohexane ring[68] produce bisignate CD signals depending on their relative orientation.

This equation provides information on the distance and relative orientation of the interacting chromophores. When TD-DFT calculations of model structures carrying two or more chromophores reproduce the observed CD signals, particularly their signal patterns, the model structures should closely resemble real structures in terms of the distance and relative orientation of the chromophores. Hence, information regarding the distance and orientation of the chromophores on the edge can be obtained from the model structures.

This concept has been applied to the structural analysis of chiral NGs. First, the edge structures of the model were optimized. The chromophores were then extracted from the optimized structures and subjected to TD-DFT calculations to obtain the CD spectra of the given distance (d_{ISD}) and orientation of the two chromophores (Fig. 17b). By removing the

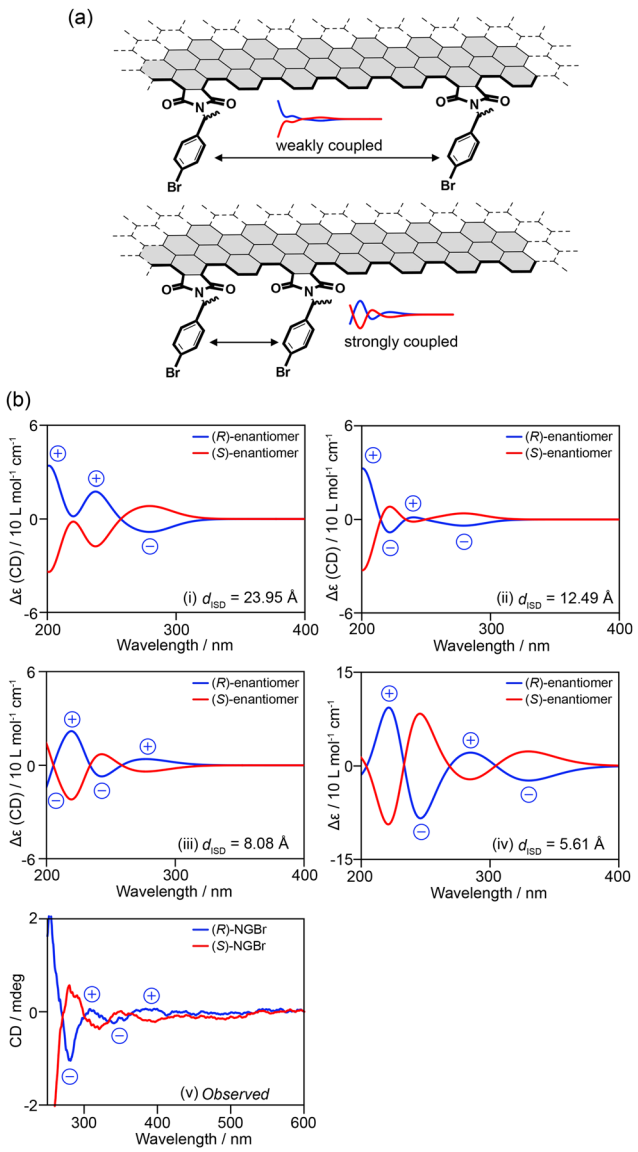

Fig. 17 (a) Concept of using exciton coupling for the structural analysis of the edge structures of NGs. (b) (i)–(iv) Calculated CD signals of model edge NGs with interchromophoric distances of (i) 23.95 Å, (ii) 12.49 Å, (iii) 8.08 Å, and (iv) 5.61 Å, and (v) observed CD signals of NGBr (ref. 71). Copyright 2024 Wiley-VCH.

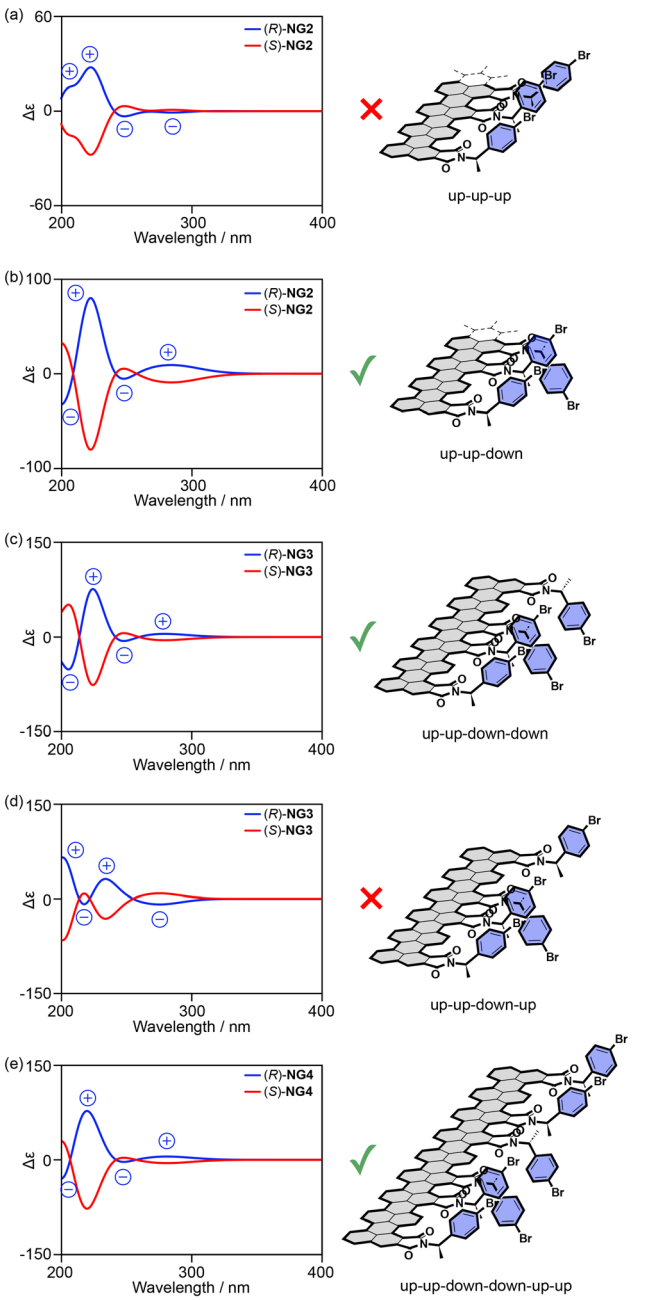

Fig. 18 (a)–(e) Calculated CD spectra of model edge structures with (a) up–up–up, (b) up–up–down, (c) up–up–down–down, (d) up–up–down–up, and (e) up–up–down–down–up–up orientations (ref. 71). Copyright 2024 Wiley-VCH.

edge from the TD-DFT calculations, the contribution of π–π* transitions on the surface was eliminated. The calculations demonstrated that when two *p*-bromophenyl groups are separated by d_{ISD} = 8.08 Å (Fig. 17b-iii), the model edge structure produced CD spectra consistent in sign with the observed ones (Fig. 17b-v). TD-DFT calculations of the model edge structures carrying three, four, and six chromophores demonstrated that when the *p*-bromophenylethyl chromophores adopt up–up–down–down alternating orientations, the model edge can reproduce the observed CD signs (Fig. 18). These observations suggest that the *p*-bromophenylethyl groups on the edge of NGBr were installed on every other armchair edge and adopted up–up–down–down alternating orientations. Moreover, the information on d_{ISD} allows us to estimate the number of functional groups attached to the NGs using the equation of $2\pi r/d_{ISD}$, where *r* is the radius of a given NG.

Structural characterization is crucial for any chemical. The nonstoichiometric mixture of top-down method-produced NGs and vast surface areas complicates the structural analysis of NG–organic hybrid materials. Although spectroscopic methods employed in the characterization of graphitic materials, such as Raman spectroscopy, XPS, NMR, and IR spectroscopy, provide evidence of the installation of functional groups, their number and orientation are difficult to determine. While the above procedure is limited to chiral NGs, combining CD spectroscopy with computational calculations provides "average" edge structures of NG–organic hybrid materials.

Conclusions

Currently, chiral NGs realized by chemical modification are still in their early stages of development. This is because these carbon frameworks are formed by oxidative cleavage of parent carbons rather than step-by-step organic synthesis, limiting the methods for inducing chirality. Some reported approaches involve introducing chiral sources at the edges to convey chiral information to the surface through steric and/or intermolecular interactions. However, the weak CD signals suggest that the induced chirality is not well rigidified and/or the chirality transfer from chiral sources anchored on the edge to the surface is inefficient. Therefore, the next stages are (1) the rigidification of the induced chirality on the surface, similar to that achieved with chiral NGs synthesized by organic synthesis, in which the carbon frameworks have a higher tolerance for racemization, and (2) the improvement of the efficiency of the chirality transfer from chiral sources to the surface. Solving these issues should allow amplification of the induced chirality and eventually realize chiral NGs with excellent chiroptical properties.

Data availability

No primary research results, software or code have been included and no new data were generated or analysed as part of this review.

Conflicts of interest

There are no conflicts to declare.

Acknowledgements

This work was supported by the Nippon Sheet Glass Foundation, Iketani Science and Technology Foundation, The Urakami Scholarship Foundation, ENEOS Tonen General Research/Development Encouragement & Scholarship Foundation, JSPS KAKENHI, Grants-in-Aid for Transformative Research Areas, "Condensed Conjugation" grant number JP21H05491 and "Materials Science of Meso-Hierarchy" grant number JP23H04873, and Grant-in-Aid for Scientific Research (A) grant number JP21H04685. We also acknowledge support from KEIRIN JKA, grant number 2023 M-419.

References

1 Y. Shen and C.-F. Chen, *Chem. Rev.*, 2012, **112**, 1463–1535.
2 A. K. Geim and K. S. Novoselov, *Nat. Mater.*, 2007, **6**, 183–191.
3 K. S. Novoselov, A. K. Geim, S. V. Morozov, D. Jiang, Y. Zhang, S. V. Dubonos, I. V. Grigorieva and A. A. Firsov, *Science*, 2004, **306**, 666–669.
4 R. Sekiya and T. Haino, *Chem. Rec.*, 2022, **22**, e202100257.
5 S. Arimura, I. Matsumoto, R. Sekiya and T. Haino, *Angew. Chem., Int. Ed.*, 2024, **63**, e202315508.
6 H. Moriguchi, R. Sekiya and T. Haino, *Small*, 2023, **19**, 202207475.
7 S. Takahashi, R. Sekiya and T. Haino, *Angew. Chem., Int. Ed.*, 2022, **61**, e202205514.
8 I. Matsumoto, R. Sekiya, H. Fukui, R. D. Sun and T. Haino, *Angew. Chem., Int. Ed.*, 2022, **61**, e202200291.
9 I. Matsumoto, R. Sekiya and T. Haino, *Angew. Chem., Int. Ed.*, 2021, **60**, 12706–12711.
10 S. Nishitani, R. Sekiya and T. Haino, *Angew. Chem., Int. Ed.*, 2020, **59**, 669–673.
11 Y. Uemura, K. Yamato, R. Sekiya and T. Haino, *Angew. Chem., Int. Ed.*, 2018, **57**, 4960–4964.
12 R. Sekiya, Y. Uemura, H. Naito, K. Naka and T. Haino, *Chem. – Eur. J.*, 2016, **22**, 8198–8206.
13 R. Sekiya, Y. Uemura, H. Murakami and T. Haino, *Angew. Chem., Int. Ed.*, 2014, **53**, 5619–5623.
14 K. Yamato, R. Sekiya, K. Suzuki and T. Haino, *Angew. Chem., Int. Ed.*, 2019, **58**, 9022–9026.
15 M. Vázquez-Nakagawa, L. Rodríguez-Pérez, N. Martín and M. A. Herranz, *Angew. Chem., Int. Ed.*, 2022, **61**, e202211365.
16 J. Ma, Y. Fu, E. Dmitrieva, F. Liu, H. Komber, F. Hennersdorf, A. A. Popov, J. J. Weigand, J. Liu and X. Feng, *Angew. Chem., Int. Ed.*, 2020, **59**, 5637–5642.

17 M. A. Medel, C. M. Cruz, D. Miguel, V. Blanco, S. P. Morcillo and A. G. Campaña, *Angew. Chem., Int. Ed.*, 2021, **60**, 22051–22056.
18 Z. Qiu, S. Asako, Y. Hu, C.-W. Ju, T. Liu, L. Rondin, D. Schollmeyer, J.-S. Lauret, K. Müllen and A. Narita, *J. Am. Chem. Soc.*, 2020, **142**, 14814–14819.
19 M. Krzeszewski, L. Dobrzycki, A. L. Sobolewski, M. K. Cyrański and D. T. Gryko, *Angew. Chem., Int. Ed.*, 2021, **60**, 14998–15005.
20 M. Roy, V. Berezhnaia, M. Villa, N. Vanthuyne, M. Giorgi, J. V. Naubron, S. Poyer, V. Monnier, L. Charles, Y. Carissan, D. Hagebaum-Reignier, J. Rodriguez, M. Gingras and Y. Coquerel, *Angew. Chem., Int. Ed.*, 2020, **59**, 3264–3271.
21 Chaolumen, I. A. Stepek, K. E. Yamada, H. Ito and K. Itami, *Angew. Chem., Int. Ed.*, 2021, **60**, 23508–23532.
22 M. A. Majewski and M. Stępień, *Angew. Chem., Int. Ed.*, 2019, **58**, 86–116.
23 Y.-J. Shen, N.-T. Yao, L.-N. Diao, Y. Yang, X.-L. Chen and H.-Y. Gong, *Angew. Chem., Int. Ed.*, 2023, **62**, e202300840.
24 J.-K. Li, X.-Y. Chen, W.-L. Zhao, Y.-L. Guo, Y. Zhang, X.-C. Wang, A. C.-H. Sue, X.-Y. Cao, M. Li, C.-F. Chen and X.-Y. Wang, *Angew. Chem., Int. Ed.*, 2023, **62**, e202215367.
25 D. Reger, P. Haines, K. Y. Amsharov, J. A. Schmidt, T. Ullrich, S. Bönisch, F. Hampel, A. Görling, J. Nelson, K. E. Jelfs, D. M. Guldi and N. Jux, *Angew. Chem., Int. Ed.*, 2021, **60**, 18073–18081.
26 M. A. Medel, R. Tapia, V. Blanco, D. Miguel, S. P. Morcillo and A. G. Campaña, *Angew. Chem., Int. Ed.*, 2021, **60**, 6094–6100.
27 Y. Chen, C. Lin, Z. Luo, Z. Yin, H. Shi, Y. Zhu and J. Wang, *Angew. Chem., Int. Ed.*, 2021, **60**, 7796–7801.
28 T. Kirschbaum, F. Rominger and M. Mastalerz, *Angew. Chem., Int. Ed.*, 2020, **59**, 270–274.
29 M. Navakouski, H. Zhylitskaya, P. J. Chmielewski, T. Lis, J. Cybinska and M. Stępień, *Angew. Chem., Int. Ed.*, 2019, **58**, 4929–4933.
30 C. M. Cruz, I. R. Márquez, S. Castro-Fernández, J. M. Cuerva, E. Maçôas and A. G. Campaña, *Angew. Chem., Int. Ed.*, 2019, **58**, 8068–8072.
31 K. Kato, Y. Segawa, L. T. Scott and K. Itami, *Angew. Chem., Int. Ed.*, 2018, **57**, 1337–1341.
32 U. Hahn, E. Maisonhaute and J.-F. Nierengarten, *Angew. Chem., Int. Ed.*, 2018, **57**, 10635–10639.
33 P. J. Evans, J. K. Ouyang, L. Favereau, J. Crassous, I. Fernández, J. Perles and N. Martín, *Angew. Chem., Int. Ed.*, 2018, **57**, 6774–6779.
34 C. M. Cruz, S. Castro-Fernández, E. Maçôas, J. M. Cuerva and A. G. Campaña, *Angew. Chem., Int. Ed.*, 2018, **57**, 14782–14786.
35 J. M. Fernández-García, P. Izquierdo-García, M. Buendía, S. Filippone and N. Martín, *Chem. Commun.*, 2022, **58**, 2634–2645.
36 Y. Dong, J. Shao, C. Chen, H. Li, R. Wang, Y. Chi, X. Lin and G. Chen, *Carbon*, 2012, **50**, 4738–4743.
37 M. A. Sk, A. Ananthanarayanan, L. Huang, K. H. Lim and P. Chen, *J. Mater. Chem. C*, 2014, **2**, 6954–6960.
38 M. Fu, F. Ehrat, Y. Wang, K. Z. Milowska, C. Reckmeier, A. L. Rogach, J. K. Stolarczyk, A. S. Urban and J. Feldmann, *Nano Lett.*, 2015, **15**, 6030–6035.
39 K. Holá, M. Sudolská, S. Kalytchuk, D. Nachtigallová, A. L. Rogach, M. Otyepka and R. Zbořil, *ACS Nano*, 2017, **11**, 12402–12410.
40 L. Li, G. Wu, G. Yang, J. Peng, J. Zhao and J.-J. Zhu, *Nanoscale*, 2013, **5**, 4015–4039.
41 S. Kim, S. W. Hwang, M.-K. Kim, D. Y. Shin, D. H. Shin, C. O. Kim, S. B. Yang, J. H. Park, E. Hwang, S.-H. Choi, G. Ko, S. Sim, C. Sone, H. J. Choi, S. Bae and B. H. Hong, *ACS Nano*, 2012, **6**, 8203–8208.
42 R. Liu, D. Wu, X. Feng and K. Müllen, *J. Am. Chem. Soc.*, 2011, **133**, 15221–15223.
43 T. Van Tam, S. G. Kang, K. F. Babu, E.-S. Oh, S. G. Lee and W. M. Choi, *J. Mater. Chem. A*, 2017, **5**, 10537–10543.
44 K. Jiang, S. Sun, L. Zhang, Y. Lu, A. Wu, C. Cai and H. Lin, *Angew. Chem., Int. Ed.*, 2015, **54**, 5360–5363.
45 C. Zhu, S. Yang, G. Wang, R. Mo, P. He, J. Sun, Z. Di, N. Yuan, J. Ding, G. Ding and X. Xie, *J. Mater. Chem. C*, 2015, **3**, 8810–8816.
46 C. Shen, S. Ge, Y. Pang, F. Xi, J. Liu, X. Dong and P. Chen, *J. Mater. Chem. B*, 2017, **5**, 6593–6600.
47 A. Ananthanarayanan, Y. Wang, P. Routh, M. A. Sk, A. Than, M. Lin, J. Zhang, J. Chen, H. Sun and P. Chen, *Nanoscale*, 2015, **7**, 8159–8165.
48 N. Sohal, B. Maity and S. Basu, *RSC Adv.*, 2021, **11**, 25586–25615.
49 L. Đorđević, F. Arcudi, A. D'Urso, M. Cacioppo, N. Micali, T. Bürgi, R. Purrello and M. Prato, *Nat. Commun.*, 2018, **9**, 3442.
50 B. Bartolomei, A. Bogo, F. Amato, G. Ragazzon and M. Prato, *Angew. Chem., Int. Ed.*, 2022, **61**, e202200038.
51 I. Matsumoto, R. Sekiya and T. Haino, *RSC Adv.*, 2019, **9**, 33843–33846.
52 C. K. Chua, Z. Sofer, P. Šimek, O. Jankovský, K. Klímová, S. Bakardjieva, S. H. Kučková and M. Pumera, *ACS Nano*, 2015, **9**, 2548–2555.
53 J. Peng, W. Gao, B. K. Gupta, Z. Liu, R. Romero-Aburto, L. H. Ge, L. Song, L. B. Alemany, X. Zhan, G. Gao, S. A. Vithayathil, B. A. Kaipparettu, A. A. Marti, T. Hayashi, J.-J. Zhu and P. M. Ajayan, *Nano Lett.*, 2012, **12**, 844–849.
54 W. S. Hummers and R. E. Offeman, *J. Am. Chem. Soc.*, 1958, **80**, 1339–1339.
55 W. Cai, R. D. Piner, F. J. Stadermann, S. Park, M. A. Shaibat, Y. Ishii, D. Yang, A. Velamakanni, S. An, M. Stoller, J. An, D. M. Chen and R. S. Ruoff, *Science*, 2008, **321**, 1815–1817.
56 J.-L. Li, K. N. Kudin, M. J. McAllister, R. K. Prud'homme, I. A. Aksay and R. Car, *Phys. Rev. Lett.*, 2006, **96**, 176101.
57 N. Fuyuno, D. Kozawa, Y. Miyauchi, S. Mouri, R. Kitaura, H. Shinohara, T. Yasuda, N. Komatsu and K. Matsuda, *Adv. Opt. Mater.*, 2014, **2**, 983–989.
58 F. Zhang, F. Liu, C. Wang, X. Xin, J. Liu, S. Guo and J. Zhang, *ACS Appl. Mater. Interfaces*, 2016, **8**, 2104–2110.

59 K. Yamato, R. Sekiya, M. Abe and T. Haino, *Chem. – Asian J.*, 2019, **14**, 1786–1791.
60 I. Matsumoto, R. Sekiya and T. Haino, *Bull. Chem. Soc. Jpn.*, 2021, **94**, 1394–1399.
61 T. Matsuo, *Bull. Chem. Soc. Jpn.*, 1964, **37**, 1844–1848.
62 S. Takahashi, R. Sekiya and T. Haino, *ChemPhysChem*, 2022, **24**, e202200465.
63 R. Sekiya and T. Haino, *Chem. – Eur. J.*, 2021, **27**, 187–199.
64 S. Arimura, I. Matsumoto, S. Nishitani, R. Sekiya and T. Haino, *Chem. – Asian J.*, 2023, **18**, e202300126.
65 N. Suzuki, Y. C. Wang, P. Elvati, Z. B. Qu, K. Kim, S. Jiang, E. Baumeister, J. Lee, B. Yeom, J. H. Bahng, J. Lee, A. Violi and N. A. Kotov, *ACS Nano*, 2016, **10**, 1744–1755.
66 M. Vázquez-Nakagawa, L. Rodríguez-Pérez, M. A. Herranz and N. Martín, *Chem. Commun.*, 2016, **52**, 665–668.
67 R. V. Person, K. Monde, H. U. Humpf, N. Berova and K. Nakanishi, *Chirality*, 1995, **7**, 128–135.
68 W. T. Wiesler, J. T. Vazquez and K. Nakanishi, *J. Am. Chem. Soc.*, 1987, **109**, 5586–5592.
69 K. Nakanishi, M. Kuroyanagi, H. Nambu, E. M. Oltz, R. Takeda, G. L. Verdine and A. Zask, *Pure Appl. Chem.*, 1984, **56**, 1031–1048.
70 S. Arimura, I. Matsumoto, S. Nishitani, R. Sekiya and T. Haino, *Chem. – Asian J.*, 2023, **18**, e202300126.
71 R. Sekiya and T. Haino, *ChemPhysChem*, 2024, **63**, e202315508.